Elastic Soil Properties From Bender Element Tests

V. M. Meyer
B.E. (Hons), Grad.IPENZ
Department of Civil and Resource Engineering, The University of Auckland, New Zealand
M. J. Pender
B.E. (Hons), PhD, FIPENZ, MASCE
Department of Civil and Resource Engineering, The University of Auckland, New Zealand
A. Nishihara
Dr. Eng., MJSCE, MJSSMFE
Department of Civil Engineering, Fukuyama University, Japan
G. C. Duske
NZCE (Civil)
Department of Civil and Resource Engineering, The University of Auckland, New Zealand

Summary This paper presents results from bender element tests performed on undisturbed samples of sand, silt and clay. The bender elements enabled both P- and S-wave velocities to be measured. Using the theory of elastic wave propagation, the dynamic elastic parameters G_{max}, E, and ν for the soil samples were evaluated. These parameters showed general agreement with soil type. Variation of these elastic parameters with test conditions, undrained shear strength and confining pressure is also presented.

1. INTRODUCTION

The three basic constants of the theory of elasticity are E, G and ν, where E is the modulus of elasticity (Young's modulus), G is the shear modulus of elasticity and ν is Poisson's ratio. These constants are essential parameters in the design and low strain analysis of many geotechnical applications. However, the non-linear inelastic behaviour of soil does not readily lend itself toward experimental determination of these elastic properties.

The very small strain shear stiffness of a soil, G_{max} or G_o, is associated with soil behaviour which is essentially elastic in nature. This condition is typically satisfied at shear strains less than 10^{-3}%, where the magnitude of the shear modulus, G, attains a constant value, G_{max}. G_{max} is commonly evaluated through dynamic in situ or laboratory testing. This paper presents the laboratory based bender element method of determining G_{max}, though the following theory is equally applicable to in situ seismic methods.

2. THEORY OF ELASTIC WAVE PROPAGATION

Seismic methods of determining G_{max} are based on the fact that the velocity at which seismic waves travel through a medium is dependent upon the elastic properties of the material. From the theory of plane wave propagation in a homogeneous isotropic elastic material, it can be shown that two principle body waves propagate. The first type is a compressional wave (P-wave), which propagates with a velocity v_p, given by:

$$v_p^2 = \frac{E(1-\nu)}{\rho(1+\nu)(1-2\nu)} \qquad (1)$$

where ρ is the mass density of the medium.

The second body wave is a shear wave (S-wave), which propagates with a velocity, v_s, given by:

$$v_s^2 = G/\rho \qquad (2)$$

Comparison of equations (1) and (2) reveals that, for the same material parameters, P-waves propagate at a much faster velocity than S-waves, with the difference between the velocities dependent upon the value of Poisson's ratio.

Measurements of v_p and v_s can be made by generating a seismic disturbance at a specific point and recording the time required for the disturbance to reach one or more receivers positioned in the medium. If the distance travelled by the body waves is known, it is possible to calculate v_p and v_s respectively. It is common practice to reverse the polarity of the seismic disturbance, which correspondingly reverses the polarity of the received signal. This enables the first arrival of the shear wave to be more clearly defined (Abbiss, 1981).

The dynamic elastic parameters G_{max}, E and ν can be evaluated if ρ, v_p and v_s of the medium are known, since:

$$G = \frac{E}{2(1+\nu)} \qquad (3)$$

Using equations (1), (2) and (3) it can be shown that:

$$\nu = \frac{\frac{1}{2}\left(V_p/V_s\right)^2 - 1}{\left(V_p/V_s\right)^2 - 1} \qquad (4)$$

A ν value approaching 0.5, corresponds to a very large bulk modulus, or a condition of zero volume change (ie an undrained test).

3. PIEZOCERAMIC BENDER ELEMENTS

A bender element is a small transducer comprised of two thin piezoceramic plates rigidly bound together in a sandwich type arrangement. The configuration of the ceramic material is such that it enables the bender element to convert electrical energy in to mechanical energy and vice-versa. Hence, an applied voltage causes the bender element to deflect a small amount, and conversely, the bender element generates a small voltage as it bends.

The use of bender elements to measure the shear wave velocity of soil in laboratory specimens has been described in detail by Shirley and Hampton (1977) and Dyvik and Madshus (1985). Test results presented in this paper were obtained by mounting bender elements in a triaxial cell using the techniques developed by Dyvik and Madshus. A brief summary of the techniques employed is given below.

The bender element must be protected from moisture to prevent electrical shorting of the

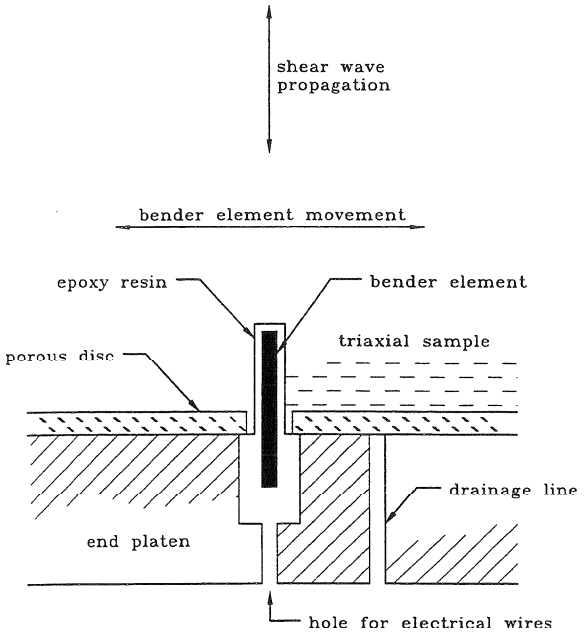

Figure 1. Bender element mounting in triaxial cell.

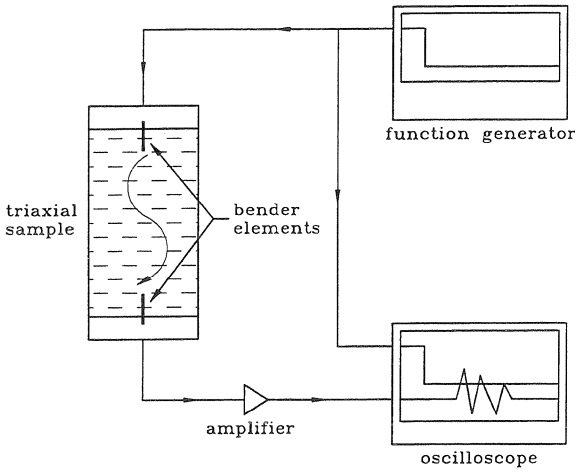

Figure 2. Schematic representation of equipment used for bender element tests.

transducer. This was achieved by encasing the bender elements in epoxy resin. The encased bender elements were then mounted in both the top and bottom end platens of a triaxial cell, as shown in Figure 1.

A porous disc with a corresponding slot could be mounted over the bender element if required. The slot in the porous disc was large enough to ensure that it did not interfere with the operation of the bender element. The resultant length of protrusion of each bender element in to the soil specimen was of the order 9.5mm with the porous disc and 11mm without.

Electrical wires connected to the bender elements were sealed in the end platens and exited the triaxial cell using pressure resistant fittings.

The bender elements were configured such that the top element could act as a transmitter and the bottom element as a receiver. Using a function generator, an electrical signal was sent to the transmitter element and the time interval until arrival at the receiver element was measured using an oscilloscope, as shown schematically in Figure 2.

4. INTERPRETATION OF BENDER ELEMENT RESULTS

Initial interpretation of bender element results is relatively straight-forward. To determine the velocity of a particle in motion (or a wave) it is necessary to know the time required for the particle to travel through a known distance. Previous test results (Dyvik and Madshus, 1985; Viggiani and Atkinson, 1995) have shown that for bender element testing the distance through which the first arrival waves travel, is the length between the tips of the bender elements. This length is commonly referred to as the *tip length* or *effective length*. Results presented in this paper confirm this observation. The time required for the waves to travel through the

effective length can be assessed as the time interval between sending the input signal to the transmitter element and the point of first arrival of the attenuated waveform at the receiver element. Figure 3 shows an idealised trace record taken from an oscilloscope. From this trace it can be observed that an initial pulse is sent to the transmitter at time, t_0, and the first arrival wave is recorded at the receiver at time, t_1. The body wave velocities, v_p and v_s, can then be defined as:

$$v_p \text{ or } v_s = {}^{l_e}/_{\Delta t} \qquad (5)$$

where l_e is the effective or tip length and Δt is the travel time for the particular wave (ie t_1-t_0).

The above method of determining body wave velocities is based on visual estimation of the time of arrival at the receiver element. This is the most commonly used method to calculate seismic wave velocities and is termed the method of *direct times of arrival*. Body wave velocities presented in this paper were determined using this method. Other methods include interval times of arrival, methods based on the cross-correlation function and methods based on dispersion curves obtained from the cross spectrum or transfer function. Viggiani and Atkinson (1995), Mancuso, Simonelli and Vinale (1989), and Sánchez-Salinero, Roesset and Stokoe (1986) present further information on these methods of analysis.

4. DIFFICULTIES ASSOCIATED WITH BENDER ELEMENT TESTING

Figure 3 is a rather idealised presentation of actual bender element results. Whilst there is general agreement that the effective wave path length is the tip length of the specimen, determination of the point of first arrival is rather more subjective, as highlighted in Figure 4. Visual methods of estimating arrival times require a degree of judgement by the observer, which is unlikely to produce exact solutions for body wave velocities. The development of mathematical/analytical methods for determining arrival times can produce solutions which are more accurate than those determined by visual methods, though it must be noted that no method is infallible. Analytical methods were developed primarily for in situ seismic testing which usually incorporate more than one receiver. Application of these methods to laboratory based bender element testing requires discretion.

4.1 Near-Field Effects

Analytical studies by Sánchez-Salinero, Roesset and Stokoe (1986) have shown that for both two-dimensional in-plane (SV-motion) and three-dimensional elasto-dynamic motion two types of body waves were present in the waveform solutions. One wave travelled at the P-wave velocity, the other at the S-wave velocity. It was observed that for S-wave excitation the amplitude of the P-wave attenuated much faster than the dominant S-wave. It was concluded that the P-wave was only significant at distances which were 'close' to the source and is commonly referred to as the *near-field wave*. The S-wave in this case is referred to as the far-field wave. Similarly, for P-wave excitation, a near-field S-wave and a far-field P-wave were observed. When the direction of the excitation impulse is reversed both the near- and far-field terms change polarity.

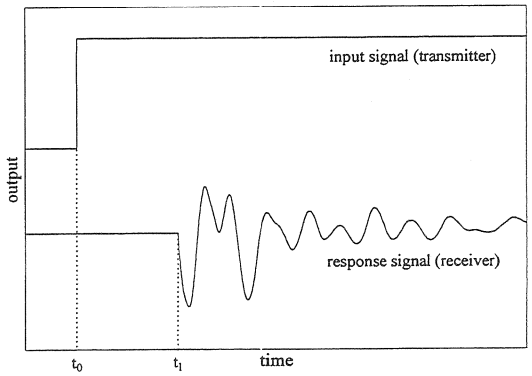

Figure 3. Idealised bender element trace record

The orientation of the bender element shown in Figure 1, is such that the element is effectively a cantilever surrounded by soil. When the bender element is excited, this configuration results in shear waves emanating from the element and propagating through the soil in a direction parallel to the axis of the specimen, ie SH-waves. Considering a bender element test of a triaxial sample as three-dimensional excitation, it is expected that a near-field P-wave will be present. The effect of this near-field wave is dependent upon the distance between the source and receiver, and consequently can mask the arrival time of the shear wave. The results presented in this paper show that the near-field P-wave can be clearly seen experimentally (Figure 4).

5. EXPERIMENTAL TEST PROCEDURES

The results presented in this paper were obtained from tests performed on samples contained in a conventional strain-controlled triaxial cell. All samples were in their natural (undisturbed) state, with nominal diameter and length of 76mm and 152mm respectively. It was necessary to pre-cut a fine slot in each end of the sample to facilitate insertion of the bender elements without damage.

Table 1. Summary of initial sample properties

Sample Number	Soil Description	Sample Depth (m)	Water Content (%)	Plastic Limit (%)	Liquid Limit (%)	Plasticity Index (%)	Bulk Density (kg/m^3)
0103 to 1004	Firm light brown silty CLAY (Waitemata Series) (avg. properties)	2.7	46.9	33.3	60.0	29.7	1700
I-0	Stiff brown highly plastic CLAY	0.5	47.6	-	-	-	1690
I-60	as for I-0	0.5	49.9	-	-	-	1710
I-90	as for I-0	0.5	51.5	-	-	-	1660
Opt1	Soft dark grey CLAY	2.9	52.3	33.0	71.0	38.0	1640
Rep2	Firm dark brown clayey SILT	2.0	53.9	-	-	-	1480
Rep3	Firm light brown silty fine SAND	5.1	50.4	-	-	-	1620

The equipment used in each bender element test included a Yokogawa FG110 2MHz synthesised function generator and a Yokogawa DL1200A 4 channel 100MHz digital oscilloscope. An amplifier (gain=56) was incorporated in the output circuit to improve readability of the received signal. From previous testing it had been observed that earthing the sample also improved the signal output.

Tests performed on each sample utilised a square pulse as an input signal, though sine pulses with frequencies in the range of 500 to 10000Hz were used with some samples. The amplitude of input signals was ±10V, which ensured an output signal of reasonable magnitude. The polarity of the input signal was reversed to assist determination of wave arrival times.

The oscilloscope permitted direct reading of time intervals using on-screen measurement cursors. Additionally, signal traces could be down-loaded directly from the oscilloscope to a personal computer for later analysis. The maximum resolution of down-loaded signals was 10000 points per channel trace.

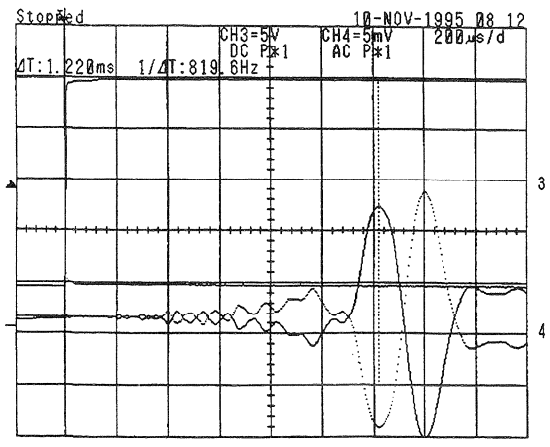

Figure 4. Square impulse (0.2ms/division).

6. TEST RESULTS

Bender element tests were performed on undisturbed samples of sand, silt and clay. A summary of sample descriptions and initial soil properties are detailed in Table 1.

Figure 4 shows a typical bender element trace record observed during sample testing. All wave velocities were determined using the method of direct times of arrival (point of first maximum reversal) and the tip length of each specimen. This trace record shows two distinct arrival times, 0.28ms and 1.22ms respectively. Considering the theory of near field effects, it is apparent that the these arrival times, T_p and T_s, correspond to a near-field P-wave and a shear wave respectively. Reversal of the polarity of the input signal correspondingly reverses the recorded output signal.

Using equations (2), (3) and (4), the dynamic elastic parameters G_{max}, E and ν were calculated for the samples tested, and are summarised in Table 2.

Figure 5 shows a plot of sample length versus travel time for differing isotropic stress states (sample 1004). It can be clearly seen that for both the S- and near-field P-waves the y-intercept is approximately 20mm, corresponding to the height of intrusion of the bender elements in the sample. This confirms the travel path of the shear (and also the near-field P-) wave is the tip length of the specimen. It should be noted, however, that the body wave velocities under zero confining stress show greater variability, with the near-field P-wave being extremely difficult to observe and is not shown in Figure 5. Bedding errors between the soil and the bender elements and incomplete saturation of the soil prior to the application of the confining stresses are possible reasons for this difficulty in observing the near-field P-wave in unconsolidated samples.

Table 2. Summary of measured soil parameters.

Sample No.	p′ (kPa)[a]	v_p (m/s)	v_s (m/s)	G_{max} (MPa)	E (MPa)	ν	s_u (kPa)
0103	10	613	72	8.9	26.6	0.493	39
0204	5	593	83	11.5	39.3	0.490	46
0302	20	579	90	13.9	41.4	0.488	47
0303	27	783	143	34.0	100.8	0.483	60
0402	100	739	114	21.7	64.6	0.488	89
0702	20	761	109	19.7	58.7	0.490	49
0703	28	700	114	21.7	64.5	0.486	60
0801	400	991	183	56.8	168.4	0.482	326
1004	46	916	122	25.6	76.3	0.491	-
I-0	0	-	116	22.6	-	-	84
I-60	0	-	108	19.7	-	-	83
I-90	0	-	108	19.3	-	-	83
Opt1	30	949	65	6.9	20.7	0.498	22
Rep2	20	762	120	21.3	63.3	0.487	138
Rep3	53	613	118	22.6	66.9	0.481	412

Three triaxial samples were trimmed from a large block sample at angles of 0°, 60° and 90° to vertical. The variation between G_{max}, s_u and the angle from vertical for samples I-0, I-60 and I-90 is presented in Figure 6. The observed trend of this plot shows that sample orientation has very little influence on G_{max} for this soil. This observation is in agreement with the trend of measured undrained shear strengths, s_u, for each sample.

Figures 7 and 8 show the variation of G_{max} and E with p′ and void ratio respectively for sample 0801. It can be observed that the dynamic elastic parameters increase with increasing confining pressure or decreasing void ratio. Viggiani and Atkinson (1995a) experimentally investigated the very small strain stiffness characteristics of fine grained soils. Results from that research proposed that G_{max} varied in accordance with p′ raised to the power of 0.6 to 0.8, dependent upon the plasticity index of the soil. Influence of the over-consolidation ratio was also taken into account.

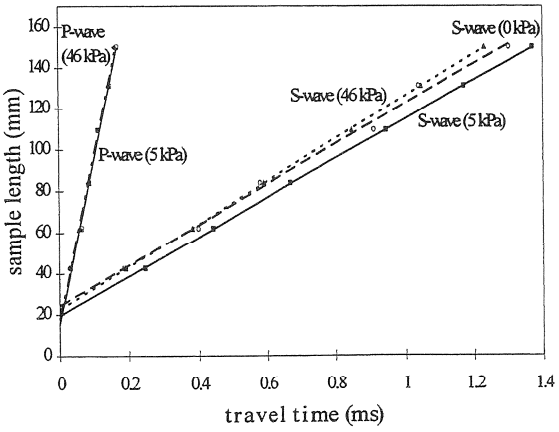

Figure 5. Wave travel time versus sample length.

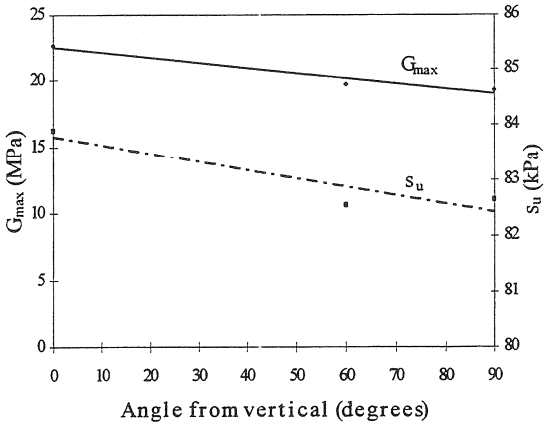

Figure 6. Variation in G_{max} with sample orientation.

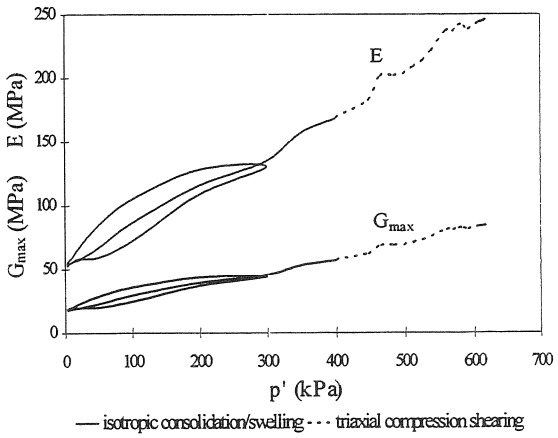

Figure 7. Variation in G_{max} and E with p′.

Such a power relationship correlates well with the data presented in this paper at higher mean stresses, though underestimates G_{max} at lower confining stresses. This is likely to be attributable to the natural bonding present in this residual soil.

[a] p′ is the mean effective stress acting on the sample

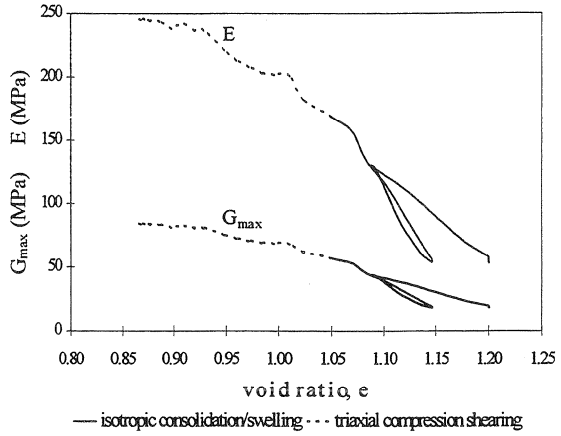

Figure 8. Variation in G_{max} and E with void ratio.

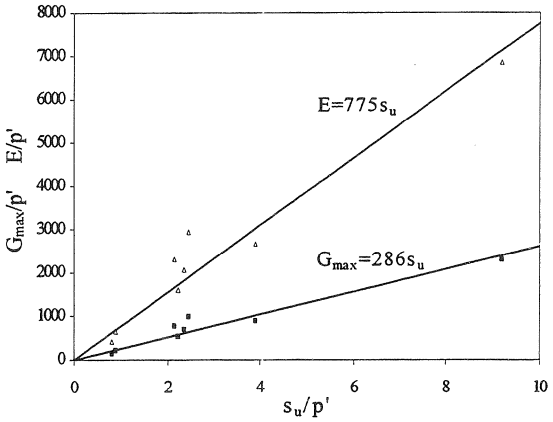

Figure 9. Variation in G_{max} and E with s_u for Waitemata Series samples.

Consequently, a linear trend more accurately fits this data for the stress range given.

Figure 9 shows the variation of G_{max} and E with the undrained shear strength, s_u, for samples taken from the Waitemata Series. Fitting linear trends to the elastic parameters results in G_{max} and E being 286 and 775 times s_u respectively.

7. CONCLUSIONS

The results have shown that it is possible to measure both P- and S-wave velocities using bender elements mounted in a triaxial cell. Knowledge of both these velocities enable the dynamic elastic parameters G_{max}, E and ν to be evaluated. For the tests presented in this paper, ν values greater than 0.48 were calculated for all samples, confirming that bender element tests measure the very small strain (elastic) properties of the soil and are essentially undrained in nature.

The P-wave velocity measured in these tests is associated with the near-field P-wave described by Sánchez-Salinero, Roesset and Stokoe (1986). To measure the P-wave velocity of a soil, it is best to use a source rich in P-waves and not rely upon a near field P-wave. However, the results presented in this paper indicate that v_p and v_s can be consistently measured for a soil specimen, enabling elastic parameters to be obtained quickly from a bender element test.

The elastic properties determined from these bender element tests show general agreement with soil type, though further work on the correlation of results with other test methods is necessary.

8. REFERENCES

Abbiss, C. P., (1981), Shear wave velocity measurements of the elasticity of the ground, *Geotechnique*, Vol. 31, No. 1, pp. 91-104.

Dyvik, R. and Madshus, C., (1985), Lab measurements of G_{max} using bender elements, *Advances in the Art of Testing Soils Under Cyclic Conditions*, Proceedings of a session of the ASCE Convention, Detroit, pp. 186-196.

Mancuso, C., Simonelli, A. L. and Vinale, F., (1989), Numerical analysis of in situ S-wave measurements, *Proceedings of the 12th International Conference on Soil Mechanics*, Vol. 3, pp. 277-280.

Sánchez-Salinero, I., Roesset, J. M. and Stokoe II, K. H., (1986), *Analytical studies of body wave propagation and attenuation*, Report GR86-15, The University of Texas at Austin.

Shirley, D. J. and Hampton, L. D., (1977), Shear wave measurements in Laboratory sediments, *Journal of the Acoustic Society of America*, Vol 63 No. 2, pp. 607-613.

Stokoe, K. H. and Woods, R. D., (1972), In situ shear wave velocity by cross-hole method, *Journal of the Soil Mechanics and Foundations Division*, ASCE, Vol. 98, No. SM 5, pp. 443-460.

Viggiani, G. and Atkinson, J. H., 1995, Interpretation of bender element tests, *Geotechnique*, Vol. 45, No. 1, pp. 149-154.

Viggiani, G. and Atkinson, J. H., 1995a, Stiffness of fine-grained soil at very small strains, *Geotechnique*, Vol. 45, No. 2, pp. 249-265.